Significance of SPDL1 as a novel prognostic factor and potential therapeutic target in clear cell renal cell carcinoma.

Klimaszewska-Wiśniewska A., Błaszczyk K., Justyna Durślewicz, Buchholz K., Jaworski D., Kwiatkowski M., Borowiak M., Grzanka D.

Supplementary Results

Protein-protein interaction network of DEGs and functional enrichment analysis

When the upregulated and downregulated DEGs were analyzed separately, high-confidence interactions occurred only between 19 of the downregulated DEGs, and these were connected by 26 edges; the remaining 35 DEGs were disconnected (clustering coefficient: 0.253; PPI enrichment p-value: < 1.2e−08; Supplementary Fig. S11A). GO-BP terms connected to cancer-related processes and overrepresented within these DEGs include regulation of chemotaxis, regulation of leukocyte migration, positive regulation of cell migration, and positive regulation of cell proliferation (Supplementary Fig. S11B). Further enrichment of these genes in GO-CC, GO-MF, KEGGs, Reactome Pathwways, Reatome Reactions, Wiki Pathways, and UniProt Immune system processes through ClueGO plugin showed their associations mostly with immune-related moleculaes and pathways, including e.g. signal transduction through IL1R, cytokine-cytokine receptor interaction, cytokine activity, IL10, IL4, IL13, IL17, IL18 signaling, regulation of T cell proliferation, regulation of leukocyte chemotaxis and migration, resistin, cells and molecule involved in local acute inflammatory response, wound healing, TLR4 signaling and tolerance, TNF signaling, LTR danger signal response pathway, altered glycosylation of MUC1 in tumor microenvironment, and prostaglandin signaling (Supplementary Fig. S11C). Furthermore, their involvement in MAPK, PI3K/AKT, and Hippo signaling pathways was also noted. The downregulated DEGs were also highly clustered in orexin receptor, phosphodiesterases (PDEs) activity, and AGE-RAGE signaling pathway (Supplementary Fig. S11C). Next, to improve connectivity of these genes and identified their close protein partners, we added no more than 15 high-confidence interactions into the 1st shell of query proteins. The resultant PPI comprised 76 nodes (of which 39 were interconneted) and 123 edges (clustering coefficient: 0.355; PPI enrichment p-value: < 1.0e−16; Supplementary Fig. S11D). The functional annotations of this PPI network using STRING and ClueGo enrichment tools showed further strengthening of the DEGs' associations with pathways and events related to immune response and immune tolerance, as well as cell migration and proliferation (Supplementary Fig. S11E, F).

The PPI network of the upregulated DEGs was loosly connected, as evidenced by a particularly small local clustering coefficient, with the vast majority of proteins being disconnected (129 nodes: 24 connected and 105 disconnected, 14 edges, LCC = 0.155, PPI enrichment p-value = 0.0002; Supplementary Fig. S12A). These genes were not enriched in any GO-BP via STRING database (data not shown). However, when re-analyzed using the ClueGO plugin for Cytoscape software, the upregulated DEGs were annotated in few GO-BP terms primarily focused on cell behavior during neuronal development, including cell adhesion, migration and secretion (Supplementary Fig. S12B). Expanding the immediate neighborhood of query proteins by 15 additional first-shell interactors resulted in the PPI network comprising 144 nodes (of which 52 were interconnected) and 74 edges (LCC = 0.258, PPI enrichment p-value = 1.33e-15; Supplementary Fig. S12C) and more functional relationships regarding cell adhesion, secretion, neuronal development, synaptic function, and negative regulation of cell locomotion (Supplementary Fig. S12D)

Supplementary figures

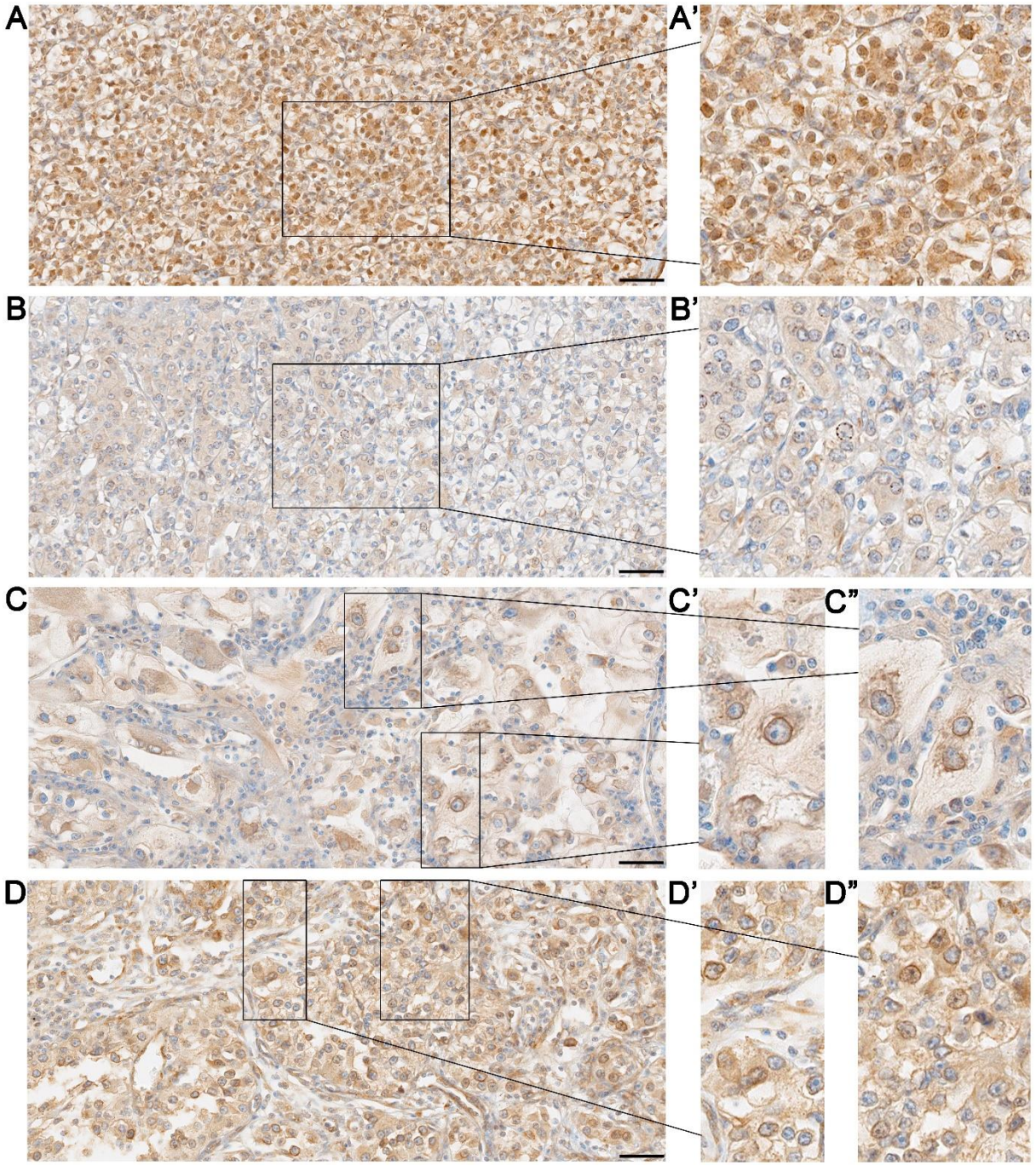

Figure S1. Representative immunohistochemically stained tissue sections of clear cell renal cell carcinomas with the focus on nuclear staining patterns of SPDL1 protein. Brown color shows SPDL1 protein, while blue color shows nuclei counterstained with hematoxylin. Bar 50 μm**.**

.

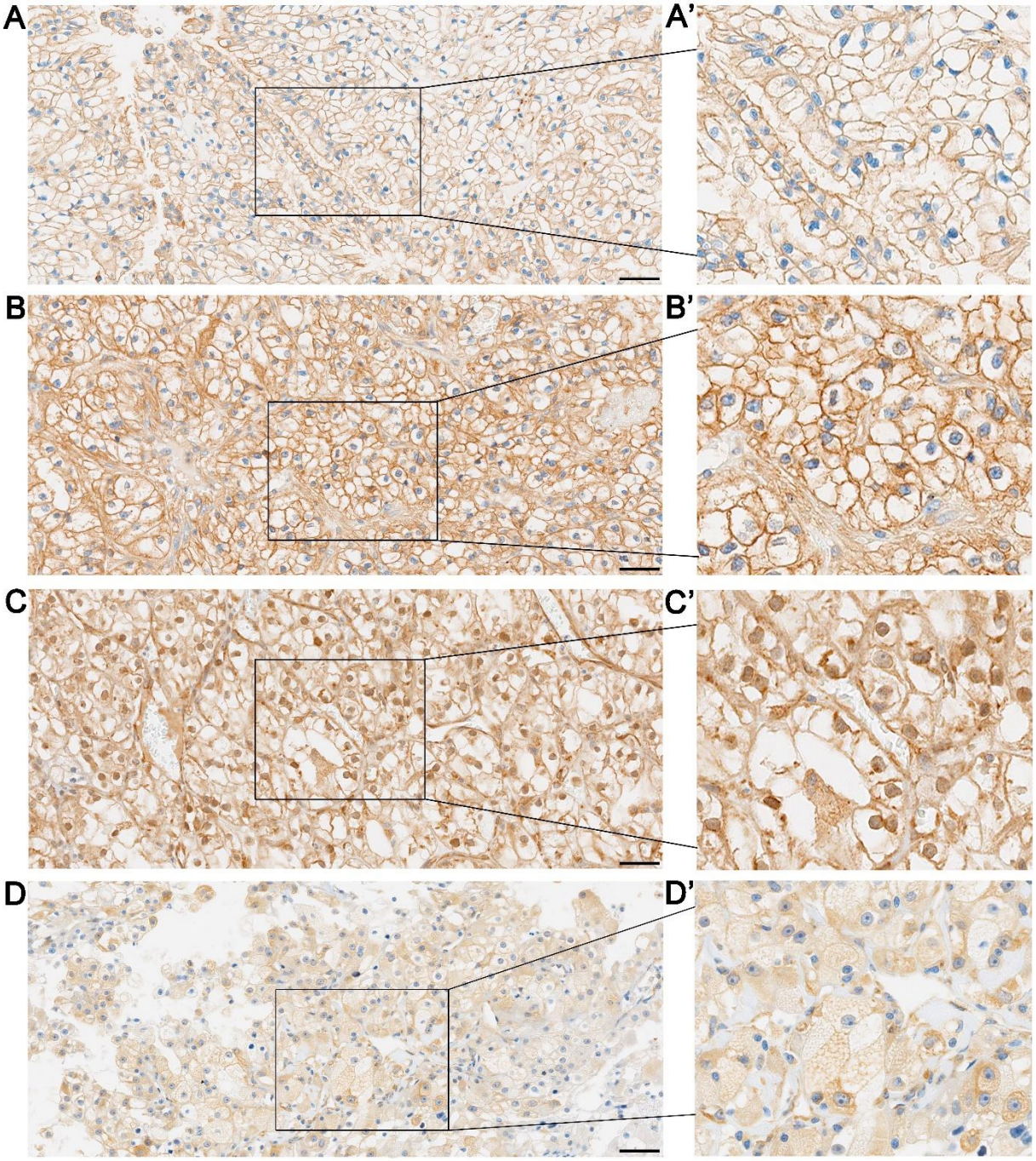

Figure S2. Representative immunohistochemically stained tissue sections of clear cell renal cell carcinomas with the focus on membranous and cytoplasmic staining patterns for SPDL1 protein. Brown color shows SPDL1 protein, while blue color shows nuclei counterstained with hematoxylin. Bar 50 μm**.**

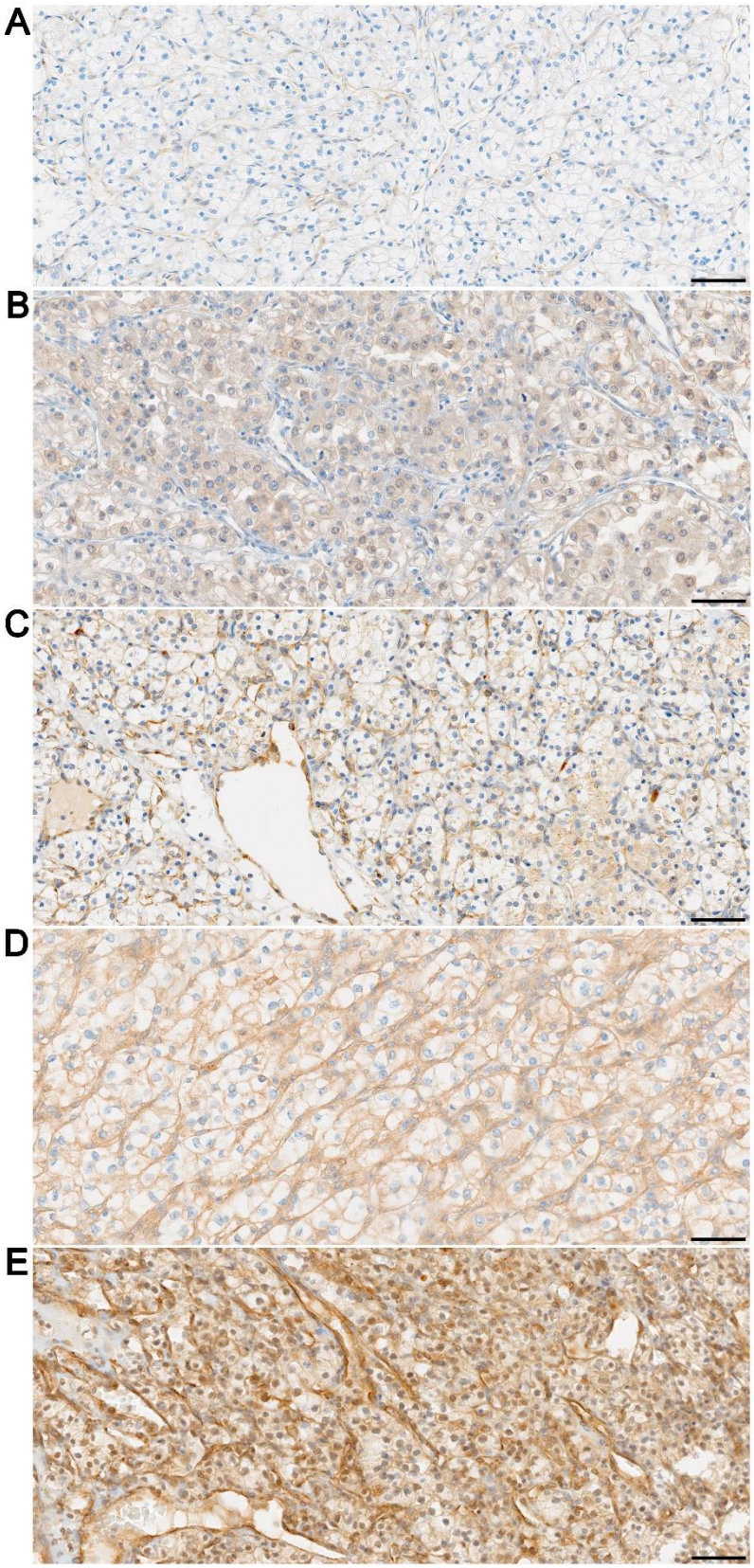

Figure S3. Representative immunohistochemically stained tissue sections of clear cell renal cell carcinomas with the focus on tumor-associated vasculature demonstrating high variability in SPDL1 expression. Brown color shows SPDL1 protein, while blue color shows nuclei counterstained with hematoxylin. Bar 50 μm**.**

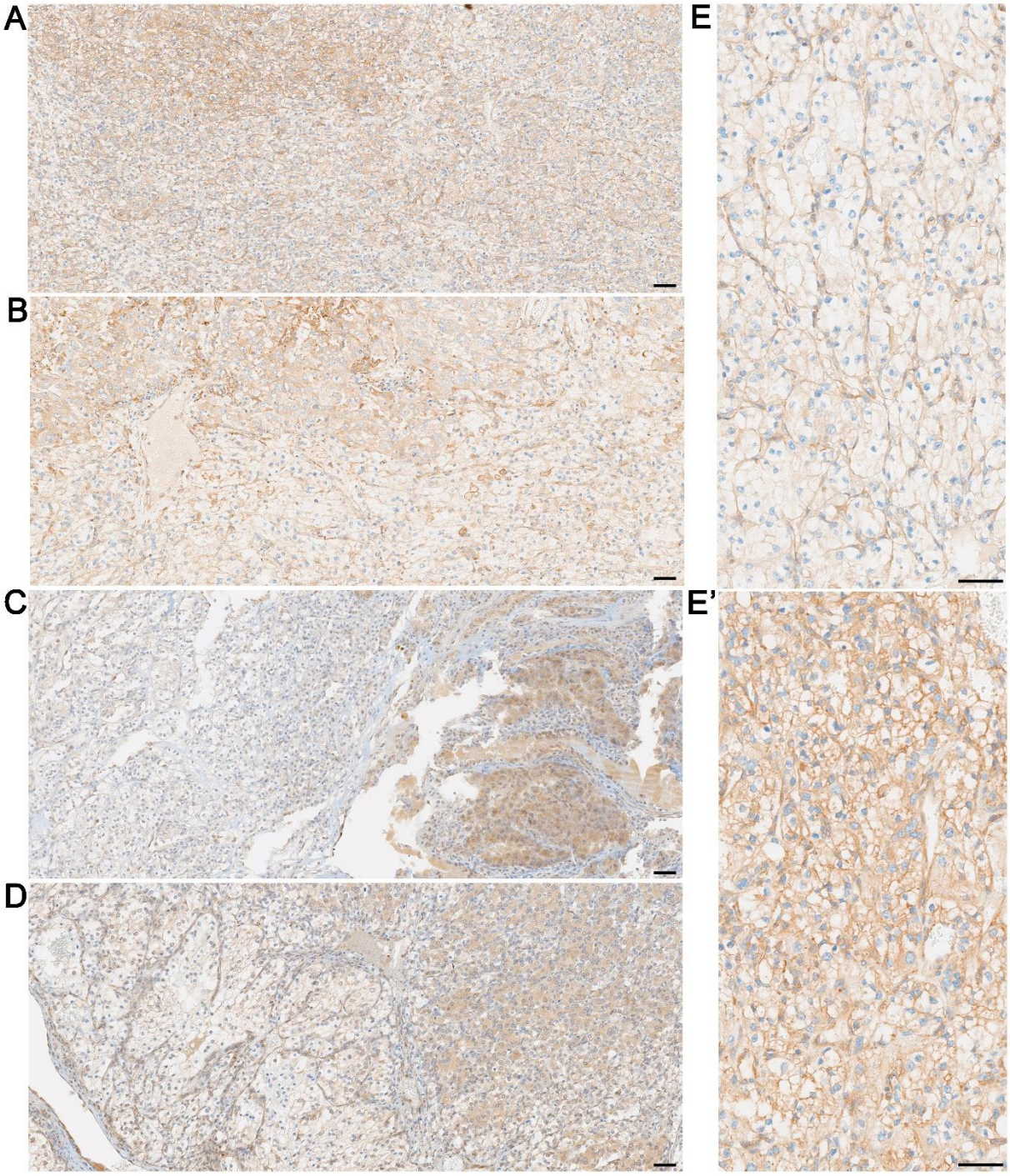

Figure S4. Representative immunohistochemically stained tissue sections of clear cell renal cell carcinomas with the focus on intratumoral heterogeneity in SPDL1 staining. Brown color shows SPDL1 protein, while blue color shows nuclei counterstained with hematoxylin. E and E' show SPDL1 staining in different tumor areas of the same patient. Bar 50 μm**.**

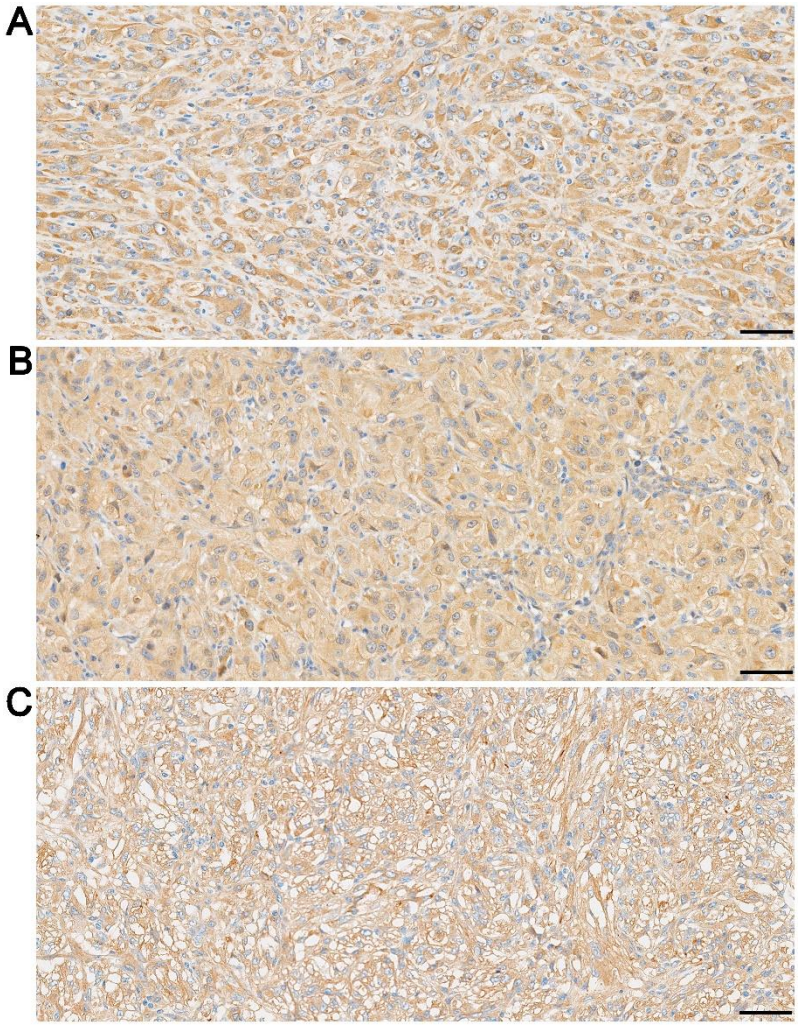

Figure S5. Representative immunohistochemically stained tissue sections of (A, B) sarcomatoid renall cell carcinoma or (C) clear cell renal cell carcinoma with sarcomatoid differentiation. Brown color shows SPDL1 protein, while blue color shows nuclei counterstained with hematoxylin. Bar 50 μm**.**

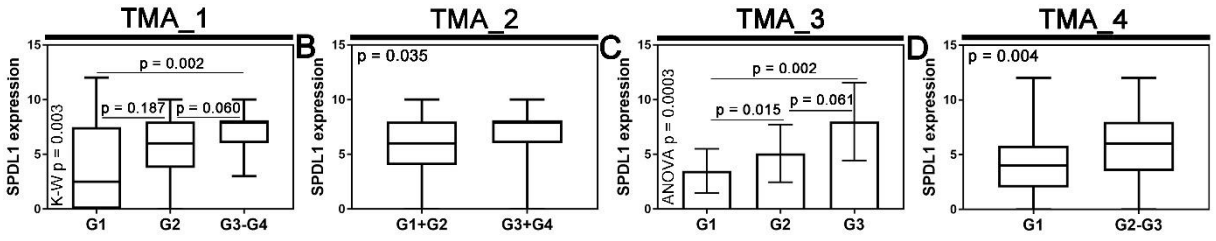

Figure S6. Expression of SPDL1 under different histological grades of clear cell renal cell carcinoma based on immunohistochemical staining. Box plots or column plots show the SPDL1 expression according to tumor grade in the tissue macro/microarray (TMA) cohorts (TMA_1 Jurasz/Bydgoszcz macroarray cohort; Błażak/Inowrocław macroarray cohort; TMA_3: KD2085 microarray cohort and TMA_4: KD2082a microarray cohort).

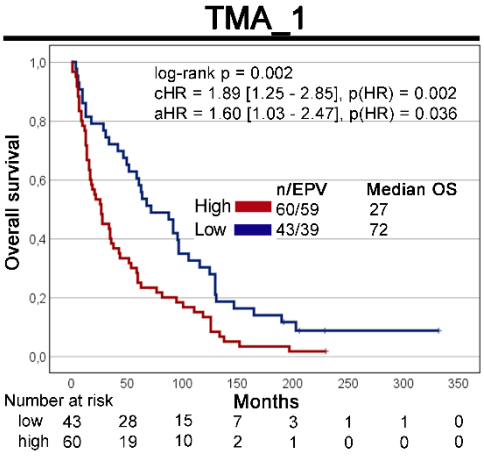

Figure S7. Effect of SPDL1 expression on overall survival in clear cell renal cell carcinoma patients stratified based on the median cut-off value. Kaplan-Meier survival curve with number at risk patients. The number of cases (n) and events per variable (EPV) for high and low expression groups is displayed. The results are displayed with the crude hazard ratio (cHR) and adjusted (aHR) from the univariable and multivariable Cox PH models, respectively, as well as the Cox *p*-values [p(HR)] and p-value from log-rank test. The 95% confidence interval is shown in square brackets. aHR is from the final multivariable Cox model with backward elimination of the nonsignificant covariates, whereby the initial model included all univariable predictors ($p < 0.05$). The median OS (in months) for high and low expression groups are also depicted. Abbreviations: OS, overall survival; TMA_1, the tissue macroarray Jurasz/Bydgoszcz cohort.

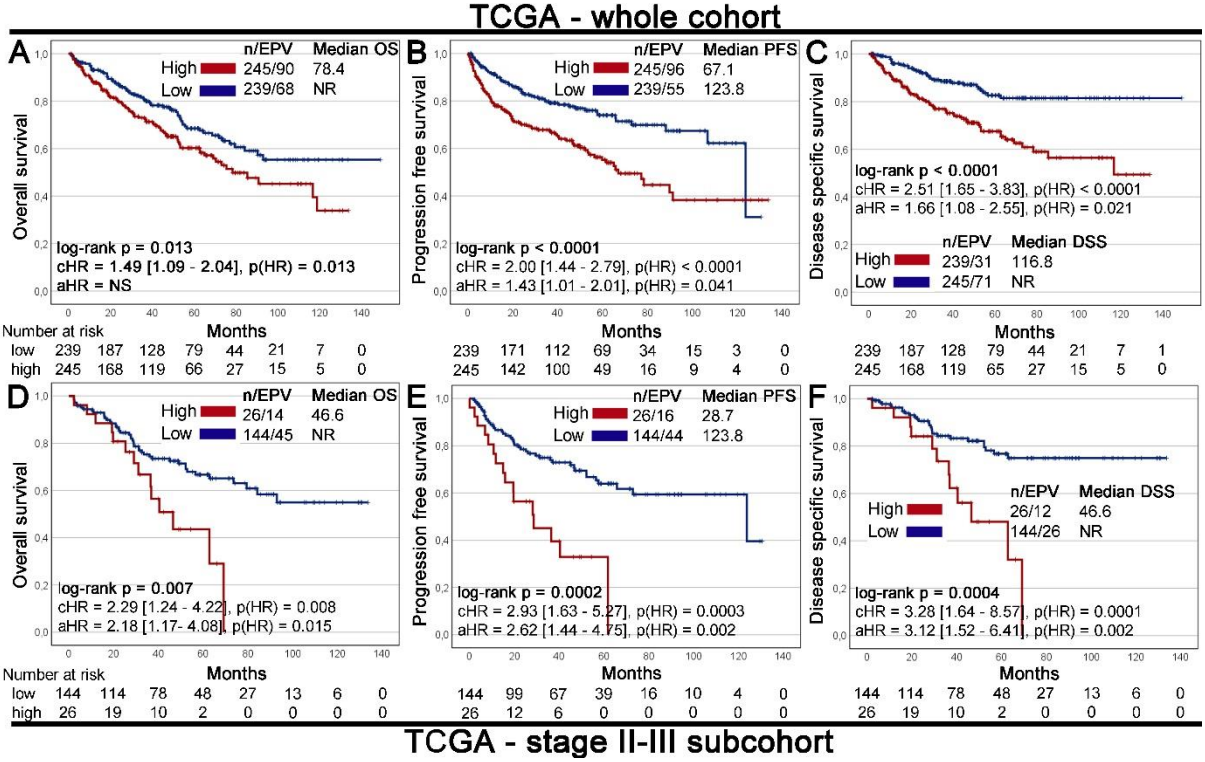

Figure S8. Effect of *SPDL1* expression on clinical outcomes in TCGA ccRCC cohort. Kaplan-Meier curves for (A, D) overall survival, (B, E) progression free survival, (C, F) disease free survival comparing high and low expression of *SPDL1* in (A-C) the whole cohort; (D-F) stage II-III subcohort. Cases were divided into low and high-expression groups according to (A-C) the median expression; (D-F) the optimal cutoff point established with the Evaluate Cutpoint software ($C_p = 9.483$). The number of cases (n) and events per variable (EPV) for low and high expression groups is shown. The results are displayed with (A-F) the crude hazard ratio (cHR) and (A-C) adjusted (aHR) from the univariable and multivariable Cox PH models, respectively, as well as (A-F) the Cox *p*-values [p(HR)] and p-value from log-rank test. The 95% confidence interval is shown in square brackets. aHR is

from the final multivariable Cox model with backward elimination of the nonsignificant covariates, whereby the initial model included all univariable predictors ($p < 0.05$). The median OS, PFS, and DSS (in months) for high and low expression groups are also depicted. Abbreviations: DSS, disease free survival; NR, not reached, NS, not significant; OS, overall survival; PFS, progression free survival; TCGA, the Cancer Genome Atlas.

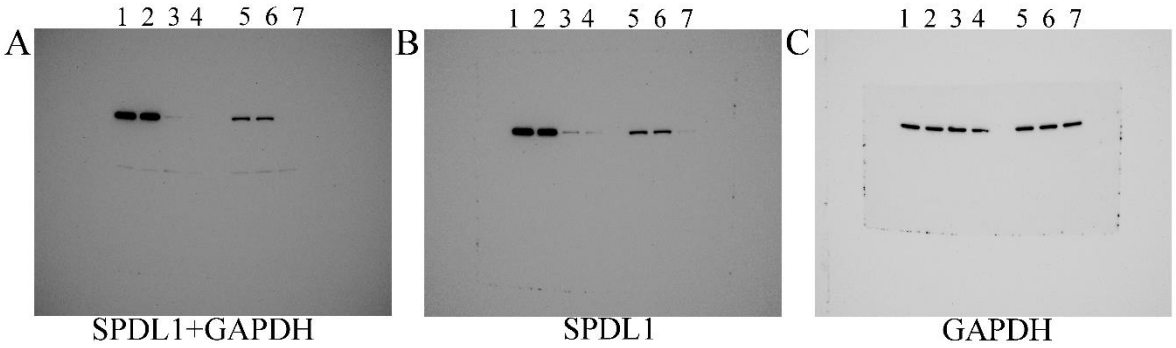

Figure S9. Full-length and separately imaged portions of the Western blot membrane showing SPDL1 expression and GAPDH as a loading control. (A) Full-length chemiluminescence image of the membrane following sequential immunodetection of SPDL1 and GAPDH using a Bio-Rad ChemiDoc imaging system. The strong SPDL1 signal limited the visual clarity of the GAPDH bands in the full-membrane image. (B, C) Separately imaged portions of the same membrane showing SPDL1 (B) and GAPDH (C), respectively, after the membrane was physically cut to separate the corresponding regions. Automatic exposure was used for all images; however, the exposure time was longer for GAPDH (C) than for SPDL1 (B) because of the weaker GAPDH signal. The full-length image is provided to document the original membrane, while panels B and C show the corresponding protein signals more clearly. Lane 1, untreated Caki-2 cells cultured under the same conditions; lane 2, Caki-2 cells transduced with scrambled shRNA (control); lane 3, Caki-2 cells transduced with *SPDL1* shRNA at a multiplicity of infection (MOI) of 2; lane 4, Caki-2 cells transduced with *SPDL1* shRNA at an MOI of 4. Lanes 5-7 show results from a separate *SPDL1* silencing experiment performed in PANC-1 cells. These data are not presented in the manuscript and are included solely to provide a complete record of the original blot.

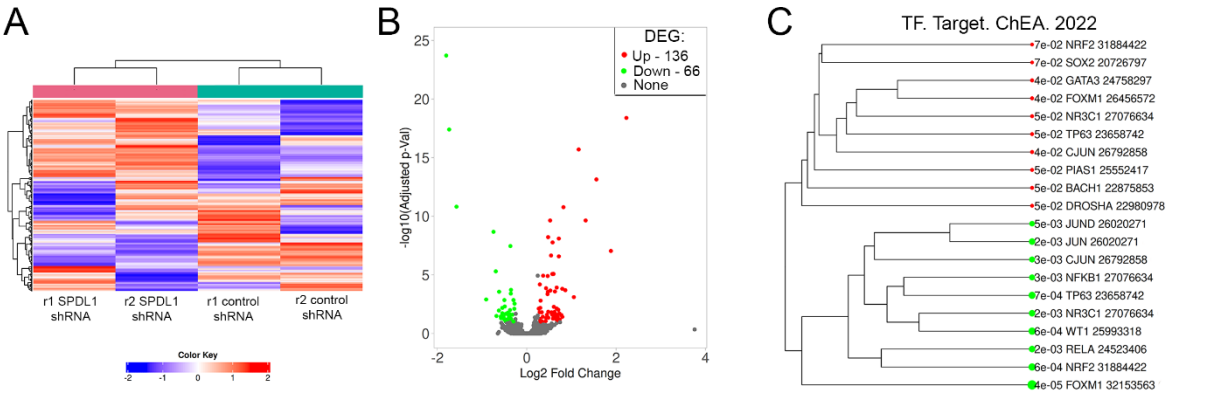

D

miRNA. Target. miRTarBase

Adj.Pval	Fold	Pathway (Click for more info)
3.09E-5	10.1	Hsa-miR-185-5p target gene
1.46E-3	10.5	Hsa-miR-4306 target gene
1.46E-3	10.3	Hsa-miR-4644 target gene
5.35E-3	24.7	Hsa-miR-1287-5p target gene
1.50E-2	18	Hsa-miR-644a target gene
4.11E-2	12.9	Hsa-miR-223-3p target gene
4.11E-2	12.8	Hsa-miR-7152-5p target gene
4.67E-2	2.9	Hsa-miR-124-3p target gene
4.67E-2	10.8	Hsa-miR-138-5p target gene
4.67E-2	10.7	Hsa-miR-5192 target gene

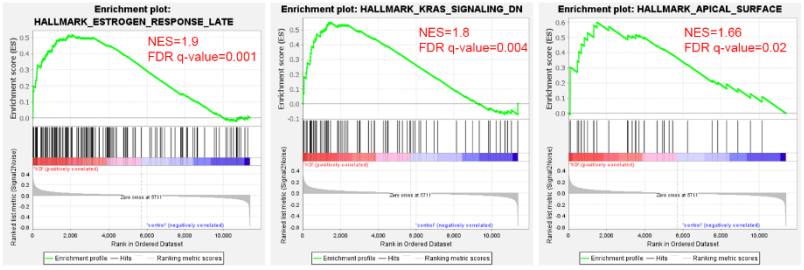

Figure S10. RNA-seq-based identification of differentially expressed genes, transcriptional and post-transcriptional regulators, and enriched gene sets. (A) Hierarchical clustering analysis of DEGs following *SPDL1* silencing in Caki-2 cells. The heatmap shows unsupervised clustering of gene expression profiles from *SPDL1* shRNA and scrambled shRNA control cells, with two independent biological replicates per condition. Samples clustered according to *SPDL1* knockdown status, demonstrating high intra-group similarity and clear separation between *SPDL1*-silenced and control cells. Gene expression values are displayed as row-scaled Z-scores. (B) Volcano plot showing differentially expressed genes (DEGs) between the *SPDL1* shRNA and scrambled shRNA control cells with selected genes marked. The red dots correspond to upregulated (-log10 (adjp) $\geq$2 and log2FC $\geq$ 0.5), and the green dots correspond to downregulated (-log10 (adjp) $\geq$2 and log2FC $\leq$ –0.05) genes. Genes without any significant differences are in grey. (C) Transcription factor enrichment analysis based on the ChEA 2022 database. Transcription factors enriched among upregulated genes are shown in red, while those enriched among downregulated genes are shown in green. Numbers displayed after each transcription factor indicate the corresponding ChEA experimental dataset identifiers. (D) miRNA enrichment analysis using the miRTarBase database revealed several miRNAs significantly enriched in *SPDL1*-silenced cells relative to scrambled shRNA controls. (E) Examples of gene sets significantly enriched in *SPDL1*-silenced cells relative to control cells, based on GSEA analysis with defined NES and FDR q-value thresholds.

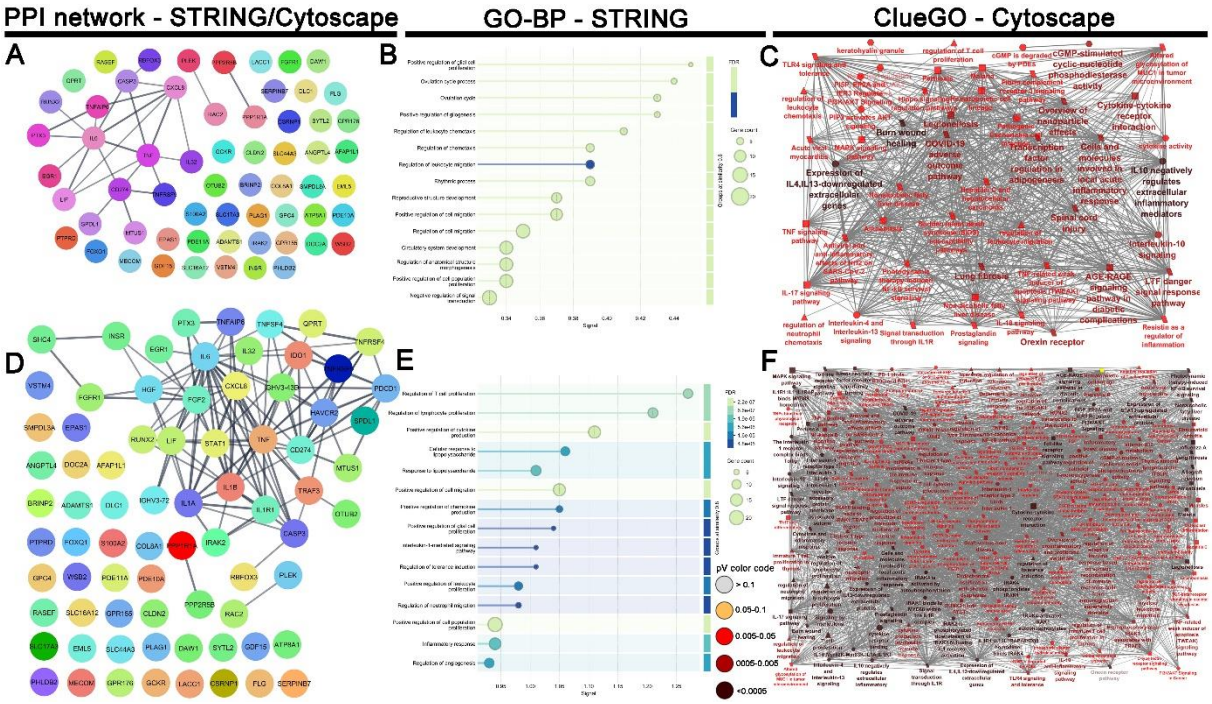

Figure S11. The STRING protein-protein interaction (PPI) analysis queried with the downregulated DEGs. Differentially expressed genes (DEGs) were identified between the Caki2-shSPDL1 and scrambled shRNA control cells. (A) The zero-order PPI network of the downregulated DEGs was constructed using the Cytoscape software; both connected and disconnected nodes are shown (B) Gene Ontology (GO) enrichment analysis of biological process (BP) for the downregulated DEGs based on STRING database with the top 15 enriched terms listed. (C) Functional analysis of the downregulated DEGs was performed by using the ClueGO plugin application available through the Cytoscape software. A network connectivity score of 0.4 and p-value cut-off $\leq$ 0.05 were used along with the GO-Cellular Component (CC), GO-Molecular Function (MF), UniProt GO-Immune system process, Reactome Pathways, Rectome Reactions, KEGG Pathways, and Wiki Pathways for the enrichment processes. (D) Extpanded PPI network was constructed using the Cytoscape software by adding no more than 15 high-confidence (0.7) interactions into the 1st shell of the downregulated DEGs; both connected and disconnected nodes are shown (E) GO-BP enrichment analysis for the downregulated DEGs and their neighboring interacting partners based on STRING database with the top 15 enriched terms listed. (F) Functional analysis of the downregulated DEGs and their 15 first-shell interactors was performed by using the ClueGO plugin application available through the Cytoscape software. A network connectivity score of 0.4 and p-value cut-off $\leq$ 0.05 were used along with the GO-CC, GO-MF, UniProt GO-Immune system process, Reactome Pathways, Rectome Reactions, KEGG Pathways, and Wiki Pathways for the enrichment processes.

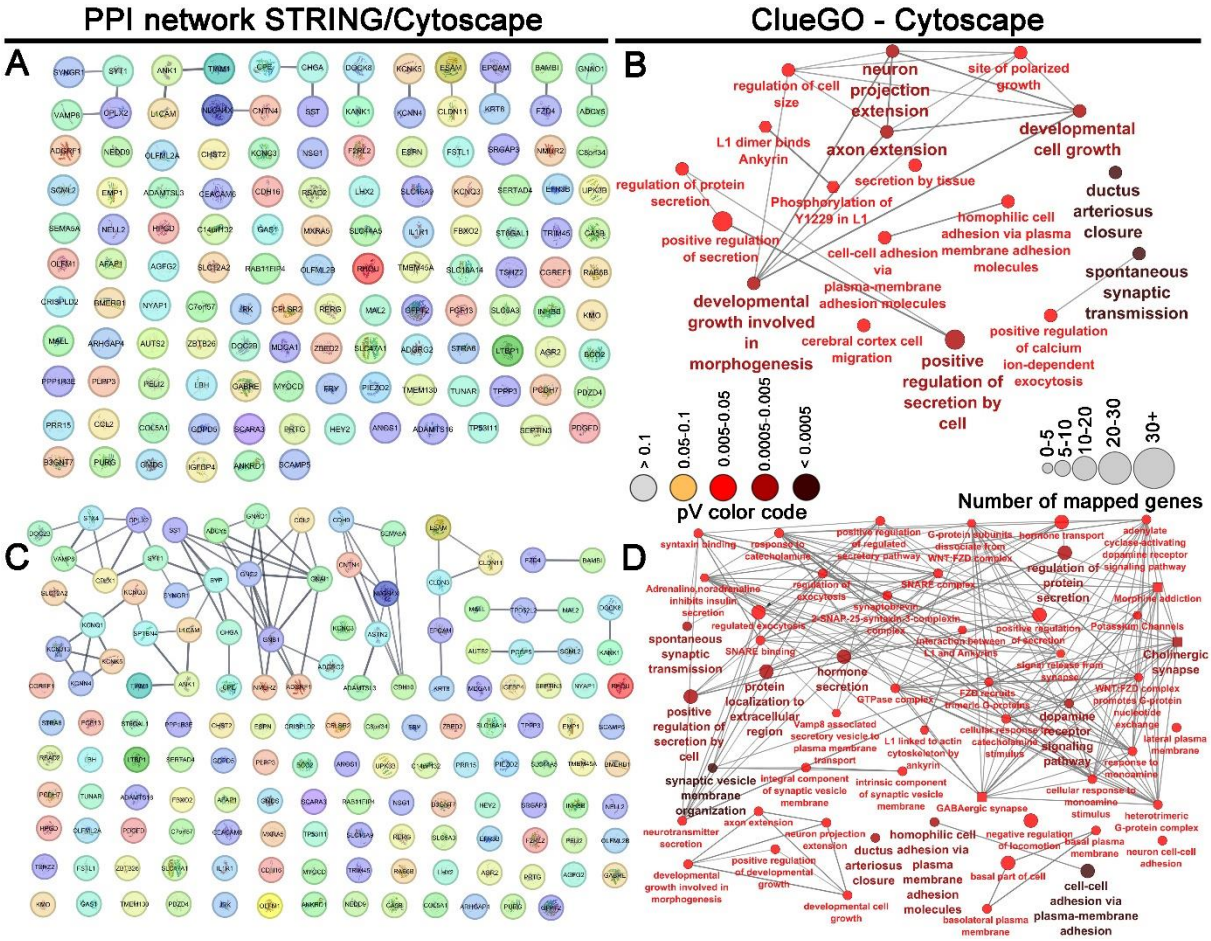

Figure S12. The STRING protein-protein interaction (PPI) analysis queried with the upregulated DEGs. Differentially expressed genes (DEGs) were identified between the Caki2-shSPDL1 and scrambled shRNA control cells. (A) The zero-order PPI network of the upregulated DEGs was constructed using the Cytoscape software; both connected and disconnected nodes are shown (B) Functional analysis of the upnregulated DEGs was performed by using the ClueGO plugin application available through the Cytoscape software. A network connectivity score of 0.4 and p-value cut-off $\leq$ 0.05 were used along with the Gene Ontology (GO) Biological Process (BP), Cellular Component (CC), Molecular Function (MF), UniProt GO-Immune system process, Reactome Pathways, Rectome Reactions, KEGG Pathways, and Wiki Pathways for the enrichment processes. (C) Extpanded PPI network was constructed using the Cytoscape software by adding no more than 15 high-confidence (0.7) interactions into the 1st shell of the upregulated DEGs; both connected and disconnected nodes are shown. (D) Functional analysis of the upregulated DEGs and their 15 first-shell interactors was performed by using the ClueGO plugin application available through the Cytoscape software. A network connectivity score of 0.4 and p-value cut-off $\leq$ 0.05 were used along with the GO-BP, GO-CC, GO-MF, UniProt GO-Immune system process, Reactome Pathways, Rectome Reactions, KEGG Pathways, and Wiki Pathways for the enrichment processes.

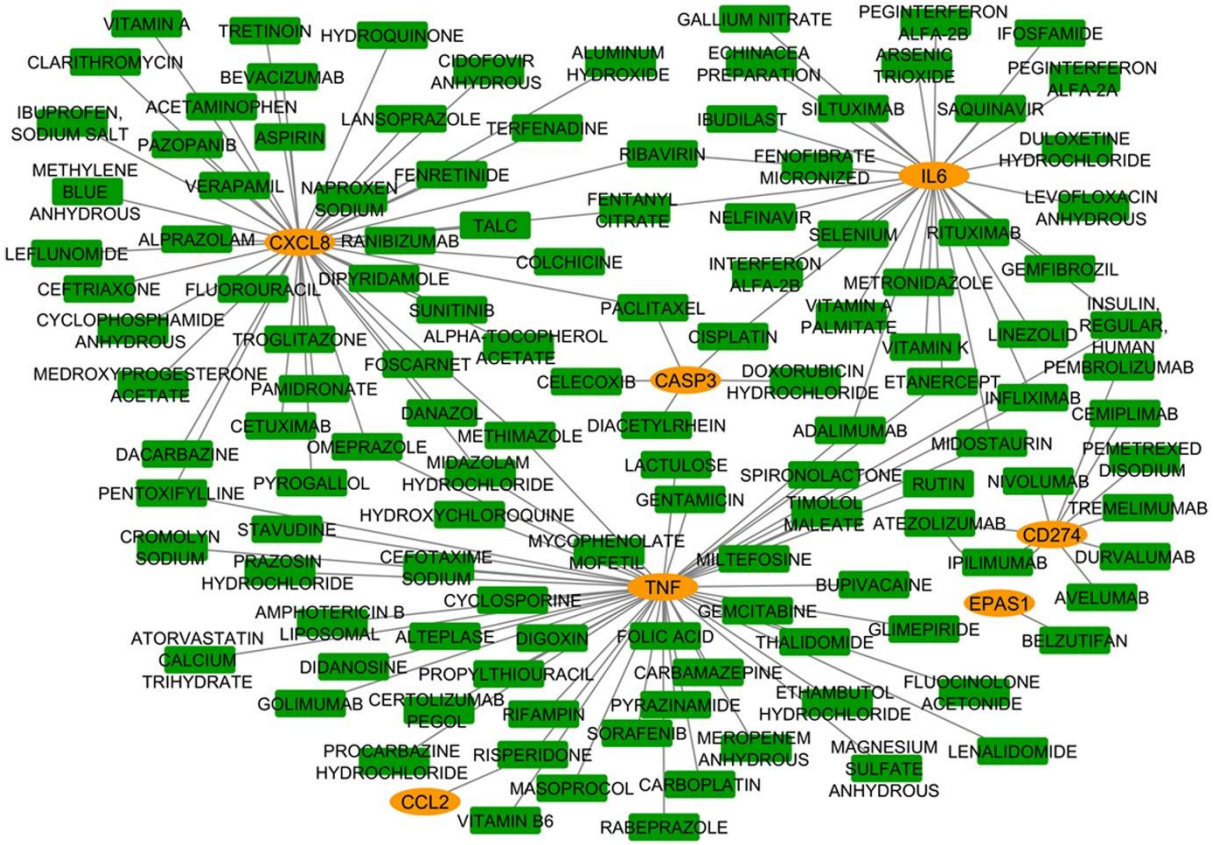

Figure S13. Candidate drugs targeting the hub genes. The candidate drug (green rectangle)-gene (orange cirle) network extracted from DGIdb database. Cytoscape software was used to visualize the network.

Supplementary Tables

Table S1. Multivariable Cox regression analysis of SPDL1 expression adjusted for each covariate individually in the TMA_1 cohort.

Variable	n/EPV	SPDL1 expression adjusted for:			
		HR	95% CI		*p*
			L	U	
Overall survival					
Age (**≥62** vs <62)	56/56_47/42	2.64	1.49	4.67	**0.0008**
Sex (**male** vs female)	69/66_34/32	3.43	1.91	6.19	**<0.0001**
Tumor grade (**G3-G4** vs G1-G2)	26/26_77/72	2.49	1.39	4.45	**0.002**
pT stage (**T3-T4** vs T1-T2)	43/40_60/58	2.85	1.62	5.02	**0.0003**
N status (**N1** vs N0)	7/7_96/91	2.73	1.55	4.80	**0.0005**
Eosinophilic cyto. (**Yes** vs No)	14/14_89/84	2.81	1.60	4.95	**0.0003**

Abbreviations: TMA – tissue macroarray; HR – hazard ratio; n – case number; EPV, events per variable, L – lower limit of the 95% confidence interval (CI), U – upper limit of the 95% confidence interval (CI).HR is shown for the SPDL1-high expression group.

Table S2. Multivariable Cox regression analysis of SPDL1 expression adjusted for each covariate individually in the TMA_2 cohort.

Variable	n/EPV	SPDL1 expression adjusted for:			
		HR	95% CI		*p*
			L	U	
Overall survival					

Age (**>57** vs ≤57)	87/37_20/2	6.35	2.47	16.36	**0.0001**
Sex **(male** vs female)	64/29_43/10	6.04	2.33	15.61	**0.0002**
Tumor grade (**G3-G4** vs G1-G2)	12/12_92/86	6.70	2.58	17.41	**0.0001**
pT stage (**T3** vs T1-T2)	18/11_89/28	5.74	2.18	15.08	**0.0004**

Abbreviations: TMA – tissue macroarray; HR – hazard ratio; n – case number; EPV, events per variable, L – lower limit of the 95% confidence interval (CI), U – upper limit of the 95% confidence interval (CI).HR is shown for the SPDL1-high expression group.

Table S3. Multivariable Cox regression analysis of *SPDL1* expression adjusted for each covariate individually in the TCGA cohort.

Variable	n/EPV	***SPDL1* expression adjusted for:**			
		HR	**95% CI**		***p***
			L	U	
Overall survival					
Age (**≥63** vs <63)	207/91_277/67	2.48	1.69	3.64	**<0.0001**
Sex **(male** vs female)	311/98_173/60	2.53	1.73	3.72	**<0.0001**
pT stage (**T3-T4** vs T1-T2)*	177/94_307/64	1.95	1.32	2.88	**0.001**
N status (**N1** vs N0)	14/9_470/149	2.34	1.59	3.46	**<0.0001**
M status (**M1** vs M0)*	73/58_411/100	1.64	1.09	2.46	**0.018**
TNM stage (**III-IV** vs I-II)	195/107_289/51	2.35	1.59	3.46	**<0.0001**
Tumor grade (**G3-G4** vs G1-G2)*	267/119_217/39	2.10	1.43	3.09	**<0.0001**
Aneuploidy score (**≥10** vs <10)	120/47_364/111	2.45	1.63	3.68	**<0.0001**
FGA (**≥0.25** vs <0.25)	92/39_392/119	2.42	1.65	3.57	**<0.0001**
Progression free survival					
Age (**≥63** vs <63)	207/75_277/76	3.47	2.39	5.05	**<0.0001**
Sex **(male** vs female)	311/107_173/44	3.51	2.42	5.10	**<0.0001**
pT stage (**T3-T4** vs T1-T2)*	177/97_307/54	2.65	1.81	3.87	**<0.0001**
N status (**N1** vs N0)	14/8_470/143	3.33	2.27	4.84	**<0.0001**
M status (**M1** vs M0)	73/64_411/87	2.07	1.41	3.06	**0.0002**
TNM stage (**III-IV** vs I-II)*	195/114_289/37	2.30	1.58	3.36	**<0.0001**
Tumor grade (**G3-G4** vs G1-G2)	267/118_217/33	2.94	2.02	4.28	**<0.0001**
Aneuploidy score (**≥10** vs <10)	120/53_364/98	3.10	2.08	4.61	**<0.0001**
FGA (**≥0.25** vs <0.25)	92/45_392/106	3.21	2.19	4.69	**<0.0001**
Disease specific survival					
Age (**≥63** vs <63)	207/53_277/49	3.56	2.32	5.47	**<0.0001**
Sex **(male** vs female)	311/70_173/32	3.55	2.31	5.45	**<0.0001**
Tumor grade (**G3-G4** vs G1-G2)	267/87_217/15	2.82	1.83	4.34	**<0.0001**
pT status (**T3-T4** vs T1-T2)	177/74_307/28	2.58	1.67	3.99	**<0.0001**
N status (**N1** vs N0)	14/7_470/95	3.32	2.14	5.14	**<0.0001**
M status (**M1** vs M0)	73/55_411/47	1.78	1.14	2.80	**0.012**
TNM stage (**III-IV** vs I-II)*	195/87_289/15	2.13	1.38	3.29	**0.0006**
Aneuploidy score (**≥10** vs <10)	120/38_364/64	3.18	2.01	5.03	**<0.0001**
FGA (**≥0.25** vs <0.25)	92/31_392/71	3.33	2.16	5.14	**<0.0001**

Abbreviations: TCGA – The Cancer Genome Atlas; HR – hazard ratio; n – case number; EPV, events per variable, L – lower limit of the 95% confidence interval (CI), U – upper limit of the 95% confidence interval (CI); FGA, fraction of genome altered. HR is shown for the *SPDL1*-high expression group. *These were added as time-dependent covariates.

Table S4. Differentially expressed genes (DEGs) between Caki2-shSPDL1 cells and shCTRL cells.

Regulation	Ensembl ID	Symbol	Type	Chr	log2 FC	Adj.Pval
Up	ENSG00000251095		lncRNA	4q22.1	2.14	2.80e-10
Up	ENSG00000157005	SST	protein_coding	3q27.3	1.90	6.65e-12
Up	ENSG00000107099	DOCK8	protein_coding	9p24.3	1.61	1.67e-12
Up	ENSG00000184613	NELL2	protein_coding	12q12	1.51	1.09e-09
Up	ENSG00000141052	MYOCD	protein_coding	17p12	1.50	1.77e-28
Up	ENSG00000213626	LBH	protein_coding	2p23.1	1.42	1.02e-81
Up	ENSG00000086548	CEACAM6	protein_coding	19q13.2	1.41	3.41e-11
Up	ENSG00000156218	ADAMTSL3	protein_coding	15q25.2	1.27	4.22e-05
Up	ENSG00000268621	IGFL2-AS1	lncRNA	19q13.32	1.27	2.73e-21
Up	ENSG00000101825	MXRA5	protein_coding	Xp22.33	1.26	3.16e-30
Up	ENSG00000084710	EFR3B	protein_coding	2p23.3	1.20	3.26e-06
Up	ENSG00000089820	ARHGAP4	protein_coding	Xq28	1.18	7.55e-10
Up	ENSG00000227051	C14orf132	protein_coding	14q32.2	1.17	3.13e-05
Up	ENSG00000119888	EPCAM	protein_coding	2p21	1.16	4.33e-07
Up	ENSG00000162745	OLFML2B	protein_coding	1q23.3	1.13	1.74e-45
Up	ENSG00000106351	AGFG2	protein_coding	7q22.1	1.11	2.65e-25
Up	ENSG00000130635	COL5A1	protein_coding	9q34.3	1.10	5.91e-22
Up	ENSG00000165449	SLC16A9	protein_coding	10q21.2	1.10	2.33e-06
Up	ENSG00000198910	L1CAM	protein_coding	Xq28	1.09	1.14e-59
Up	ENSG00000163053	SLC16A14	protein_coding	2q36.3	1.09	3.72e-07
Up	ENSG00000095739	BAMBI	protein_coding	10p12.1	1.08	3.84e-19
Up	ENSG00000134533	RERG	protein_coding	12p12.3	1.06	5.47e-06
Up	ENSG00000137868	STRA6	protein_coding	15q24.1	1.05	5.81e-16
Up	ENSG00000011201	ANOS1	protein_coding	Xp22.31	1.04	4.63e-20
Up	ENSG00000187017	ESPN	protein_coding	1p36.31	1.03	1.86e-15
Up	ENSG00000137968	SLC44A5	protein_coding	1p31.1	1.02	3.00e-07
Up	ENSG00000185585	OLFML2A	protein_coding	9q33.3	0.99	2.17e-08
Up	ENSG00000164120	HPGD	protein_coding	4q34.1	0.97	1.31e-03
Up	ENSG00000267519	MIR23AHG	lncRNA	19p13.12	0.94	5.85e-05
Up	ENSG00000163430	FSTL1	protein_coding	3q13.33	0.94	8.07e-04
Up	ENSG00000135547	HEY2	protein_coding	6q22.31	0.93	5.50e-04
Up	ENSG00000164626	KCNK5	protein_coding	6p21.2	0.91	5.69e-03
Up	ENSG00000176532	PRR15	protein_coding	7p14.3	0.90	2.85e-06
Up	ENSG00000111859	NEDD9	protein_coding	6p24.2	0.90	4.02e-05
Up	ENSG00000184156	KCNQ3	protein_coding	8q24.22	0.89	9.44e-08
Up	ENSG00000116574	RHOU	protein_coding	1q42.13	0.88	4.37e-03
Up	ENSG00000115594	IL1R1	protein_coding	2q11.2	0.87	8.14e-03
Up	ENSG00000106541	AGR2	protein_coding	7p21.1	0.87	8.44e-04
Up	ENSG00000156299	TIAM1	protein_coding	21q22.11	0.86	3.46e-03
Up	ENSG00000130558	OLFM1	protein_coding	9q34.3	0.86	5.99e-04
Up	ENSG00000112139	MDGA1	protein_coding	6p21.2	0.85	4.45e-22
Up	ENSG00000131459	GFPT2	protein_coding	5q35.3	0.85	7.30e-03
Up	ENSG00000173698	ADGRG2	protein_coding	Xp22.13	0.84	1.56e-65
Up	ENSG00000163083	INHBB	protein_coding	2q14.2	0.83	1.00e-22
Up	ENSG00000177494	ZBED2	protein_coding	3q13.13	0.83	9.28e-09
Up	ENSG00000227121	LINC02672	lncRNA	10q21.1	0.83	6.88e-05
Up	ENSG00000250366	TUNAR	protein_coding	14q32.2	0.83	1.51e-07
Up	ENSG00000266976		lncRNA	19q12	0.82	6.68e-03
Up	ENSG00000168824	NSG1	protein_coding	4p16.3	0.81	1.17e-03
Up	ENSG00000243566	UPK3B	protein_coding	7q11.23	0.81	1.99e-02
Up	ENSG00000182463	TSHZ2	protein_coding	20q13.2	0.81	5.28e-04
Up	ENSG00000271122	HERPUD2-AS1	lncRNA	7p14.2	0.81	2.20e-03
Up	ENSG00000175274	TP53I11	protein_coding	11p11.2	0.81	1.06e-07
Up	ENSG00000149564	ESAM	protein_coding	11q24.2	0.80	6.74e-07
Up	ENSG00000146938	NLGN4X	protein_coding	Xp22.31	0.80	1.42e-13
Up	ENSG00000141753	IGFBP4	protein_coding	17q21.2	0.79	5.03e-47
Up	ENSG00000170962	PDGFD	protein_coding	11q22.3	0.78	2.66e-12
Up	ENSG00000107104	KANK1	protein_coding	9p24.3	0.78	9.82e-33

Up	ENSG00000159713	TPPP3	protein_coding	16q22.1	0.77	1.25e-04
Up	ENSG00000173175	ADCY5	protein_coding	3q21.1	0.77	9.28e-10
Up	ENSG00000164746	C7orf57	protein_coding	7p12.3	0.77	1.23e-02
Up	ENSG00000118640	VAMP8	protein_coding	2p11.2	0.77	1.55e-02
Up	ENSG00000116661	FBXO2	protein_coding	1p36.22	0.77	8.40e-04
Up	ENSG00000275216		lncRNA	13q33.3	0.77	2.09e-28
Up	ENSG00000087258	GNAO1	protein_coding	16q13	0.76	2.75e-03
Up	ENSG00000049323	LTBP1	protein_coding	2p22.3	0.76	9.08e-06
Up	ENSG00000197580	BCO2	protein_coding	11q23.1	0.75	2.80e-06
Up	ENSG00000283265		lncRNA	6q23.3	0.75	2.63e-03
Up	ENSG00000103196	CRISPLD2	protein_coding	16q24.1	0.75	1.07e-05
Up	ENSG00000145536	ADAMTS16	protein_coding	5p15.32	0.75	5.56e-09
Up	ENSG00000175040	CHST2	protein_coding	3q24	0.75	3.97e-05
Up	ENSG00000129682	FGF13	protein_coding	Xq27.1	0.75	1.43e-02
Up	ENSG00000225138	SLC9A3-AS1	lncRNA	5p15.33	0.74	1.29e-02
Up	ENSG00000100167	SEPTIN3	protein_coding	22q13.2	0.74	8.60e-07
Up	ENSG00000234616	JRK	protein_coding	8q24.3	0.73	4.75e-08
Up	ENSG00000109472	CPE	protein_coding	4q32.3	0.73	6.88e-04
Up	ENSG00000198743	SLC5A3	protein_coding	21q22.11	0.72	9.04e-27
Up	ENSG00000196220	SRGAP3	protein_coding	3p25.3	0.72	1.48e-07
Up	ENSG00000082497	SERTAD4	protein_coding	1q32.2	0.72	5.99e-03
Up	ENSG00000144063	MALL	protein_coding	2q13	0.72	1.20e-12
Up	ENSG00000102287	GABRE	protein_coding	Xq28	0.72	4.56e-02
Up	ENSG00000169851	PCDH7	protein_coding	4p15.1	0.72	1.58e-20
Up	ENSG00000148677	ANKRD1	protein_coding	10q23.31	0.72	4.13e-03
Up	ENSG00000117009	KMO	protein_coding	1q43	0.71	4.63e-02
Up	ENSG00000162407	PLPP3	protein_coding	1p32.2	0.70	1.56e-02
Up	ENSG00000172733	PURG	protein_coding	8p12	0.70	2.17e-06
Up	ENSG00000064651	SLC12A2	protein_coding	5q23.3	0.70	1.03e-15
Up	ENSG00000174804	FZD4	protein_coding	11q14.2	0.69	1.02e-02
Up	ENSG00000235194	PPP1R3E	protein_coding	14q11.2	0.69	1.75e-02
Up	ENSG00000154864	PIEZO2	protein_coding	18p11.21	0.69	1.90e-09
Up	ENSG00000112699	GMDS	protein_coding	6p25.3	0.69	5.47e-06
Up	ENSG00000134321	RSAD2	protein_coding	2p25.2	0.69	2.20e-03
Up	ENSG00000166924	NYAP1	protein_coding	7q22.1	0.68	3.07e-02
Up	ENSG00000100604	CHGA	protein_coding	14q32.12	0.68	2.86e-24
Up	ENSG00000067840	PDZD4	protein_coding	Xq28	0.68	2.13e-02
Up	ENSG00000196526	AFAP1	protein_coding	4p16.1	0.68	1.48e-06
Up	ENSG00000144619	CNTN4	protein_coding	3p26.3	0.68	1.50e-03
Up	ENSG00000169239	CA5B	protein_coding	Xp22.2	0.67	9.29e-04
Up	ENSG00000073849	ST6GAL1	protein_coding	3q27.3	0.67	7.14e-18
Up	ENSG00000102098	SCML2	protein_coding	Xp22.13	0.67	5.99e-03
Up	ENSG00000145920	CPLX2	protein_coding	5q35.2	0.66	1.32e-03
Up	ENSG00000198794	SCAMP5	protein_coding	15q24.2	0.66	1.78e-02
Up	ENSG00000166450	PRTG	protein_coding	15q21.3	0.65	1.92e-04
Up	ENSG00000134531	EMP1	protein_coding	12p13.1	0.65	1.24e-11
Up	ENSG00000223764	LINC02593	lncRNA	1p36.33	0.65	2.49e-02
Up	ENSG00000166589	CDH16	protein_coding	16q22.1	0.65	1.05e-15
Up	ENSG00000153292	ADGRF1	protein_coding	6p12.3	0.64	2.59e-24
Up	ENSG00000108691	CCL2	protein_coding	17q12	0.64	4.85e-02
Up	ENSG00000180447	GAS1	protein_coding	9q21.33	0.64	1.64e-02
Up	ENSG00000154917	RAB6B	protein_coding	3q22.1	0.64	4.53e-02
Up	ENSG00000158555	GDPD5	protein_coding	11q13.5	0.63	2.62e-02
Up	ENSG00000106689	LHX2	protein_coding	9q33.3	0.63	2.18e-04
Up	ENSG00000168077	SCARA3	protein_coding	8p21.1	0.63	2.50e-11
Up	ENSG00000170421	KRT8	protein_coding	12q13.13	0.63	2.47e-42
Up	ENSG00000067715	SYT1	protein_coding	12q21.2	0.62	5.87e-11
Up	ENSG00000073910	FRY	protein_coding	13q13.1	0.62	1.81e-02
Up	ENSG00000166448	TMEM130	protein_coding	7q22.1	0.62	1.72e-13
Up	ENSG00000132911	NMUR2	protein_coding	5q33.1	0.62	1.30e-06

Up	ENSG00000013297	CLDN11	protein_coding	3q26.2	0.62	1.00e-02
Up	ENSG00000143126	CELSR2	protein_coding	1p13.3	0.62	1.50e-17
Up	ENSG00000100321	SYNGR1	protein_coding	22q13.1	0.62	5.15e-06
Up	ENSG00000134253	TRIM45	protein_coding	1p13.1	0.62	2.22e-03
Up	ENSG00000181458	TMEM45A	protein_coding	3q12.2	0.62	4.37e-04
Up	ENSG00000261713	SSTR5-AS1	lncRNA	16p13.3	0.62	2.20e-02
Up	ENSG00000131242	RAB11FIP4	protein_coding	17q11.2	0.61	2.20e-03
Up	ENSG00000156966	B3GNT7	protein_coding	2q37.1	0.61	5.13e-03
Up	ENSG00000165084	C8orf34	protein_coding	8q13.2	0.61	3.58e-04
Up	ENSG00000138028	CGREF1	protein_coding	2p23.3	0.61	9.22e-03
Up	ENSG00000142494	SLC47A1	protein_coding	17p11.2	0.61	4.77e-03
Up	ENSG00000131398	KCNC3	protein_coding	19q13.33	0.60	6.91e-03
Up	ENSG00000272636	DOC2B	protein_coding	17p13.3	0.60	2.72e-03
Up	ENSG00000104783	KCNN4	protein_coding	19q13.31	0.60	1.97e-02
Up	ENSG00000166780	BMERB1	protein_coding	16p13.11	0.60	4.28e-09
Up	ENSG00000112902	SEMA5A	protein_coding	5p15.31	0.60	2.59e-02
Up	ENSG00000139946	PELI2	protein_coding	14q22.3	0.60	4.09e-03
Up	ENSG00000029534	ANK1	protein_coding	8p11.21	0.59	8.50e-04
Up	ENSG00000171448	ZBTB26	protein_coding	9q33.2	0.59	1.34e-02
Up	ENSG00000147676	MAL2	protein_coding	8q24.12	0.59	5.75e-04
Up	ENSG00000164220	F2RL2	protein_coding	5q13.3	0.59	8.75e-04
Up	ENSG00000158321	AUTS2	protein_coding	7q11.22	0.59	2.89e-04
Down	ENSG00000259001		lncRNA	14q11.2	-2.04	3.04e-289
Down	ENSG00000166396	SERPINB7	protein_coding	18q21.33	-1.79	2.56e-10
Down	ENSG00000124564	SLC17A3	protein_coding	6p22.2	-1.70	7.95e-13
Down	ENSG00000040275	SPDL1	protein_coding	5q35.1	-1.58	6.10e-102
Down	ENSG00000136244	IL6	protein_coding	7p15.3	-1.57	3.27e-17
Down	ENSG00000123610	TNFAIP6	protein_coding	2q23.3	-1.26	1.02e-13
Down	ENSG00000152779	SLC16A12	protein_coding	10q23.31	-1.20	4.61e-09
Down	ENSG00000120738	EGR1	protein_coding	5q31.2	-1.10	2.70e-02
Down	ENSG00000115956	PLEK	protein_coding	2p14	-1.10	1.47e-10
Down	ENSG00000198797	BRINP2	protein_coding	1q25.2	-1.08	5.20e-04
Down	ENSG00000237975	FLG-AS1	lncRNA	1q21.3	-1.08	1.64e-05
Down	ENSG00000165376	CLDN2	protein_coding	Xq22.3	-1.07	1.23e-19
Down	ENSG00000169429	CXCL8	protein_coding	4q13.3	-1.07	6.21e-05
Down	ENSG00000289901	NA	NA	NANA	-1.02	1.40e-05
Down	ENSG00000008517	IL32	protein_coding	16p13.3	-1.00	6.89e-27
Down	ENSG00000143631	FLG	protein_coding	1q21.3	-1.00	5.75e-05
Down	ENSG00000049249	TNFRSF9	protein_coding	1p36.23	-0.98	2.81e-03
Down	ENSG00000166073	GPR176	protein_coding	15q15.1	-0.97	6.19e-07
Down	ENSG00000163328	GPR155	protein_coding	2q31.1	-0.87	7.52e-03
Down	ENSG00000181690	PLAG1	protein_coding	8q12.1	-0.85	1.69e-03
Down	ENSG00000232810	TNF	protein_coding	6p21.33	-0.84	1.69e-03
Down	ENSG00000089723	OTUB2	protein_coding	14q32.12	-0.82	1.98e-08
Down	ENSG00000165633	VSTM4	protein_coding	10q11.23	-0.80	1.97e-06
Down	ENSG00000123977	DAW1	protein_coding	2q36.3	-0.79	1.47e-02
Down	ENSG00000134070	IRAK2	protein_coding	3p25.3	-0.79	1.80e-06
Down	ENSG00000179630	LACC1	protein_coding	13q14.11	-0.78	1.62e-02
Down	ENSG00000214900	LINC01588	lncRNA	14q21.3	-0.76	3.66e-03
Down	ENSG00000167281	RBFOX3	protein_coding	17q25.3	-0.75	3.88e-04
Down	ENSG00000068971	PPP2R5B	protein_coding	11q13.1	-0.74	1.42e-05
Down	ENSG00000153707	PTPRD	protein_coding	9p23	-0.73	6.15e-03
Down	ENSG00000112541	PDE10A	protein_coding	6q27	-0.72	1.12e-07
Down	ENSG00000128655	PDE11A	protein_coding	2q31.2	-0.72	1.84e-03
Down	ENSG00000120217	CD274	protein_coding	9p24.1	-0.72	5.68e-06
Down	ENSG00000143036	SLC44A3	protein_coding	1p21.3	-0.71	1.64e-02
Down	ENSG00000165521	EML5	protein_coding	14q31.3	-0.71	3.56e-02
Down	ENSG00000144655	CSRNP1	protein_coding	3p22.2	-0.70	3.41e-02
Down	ENSG00000149927	DOC2A	protein_coding	16p11.2	-0.70	1.27e-04
Down	ENSG00000164379	FOXQ1	protein_coding	6p25.3	-0.70	2.99e-12

Down	ENSG00000124406	ATP8A1	protein_coding	4p13	-0.70	6.88e-03
Down	ENSG00000130513	GDF15	protein_coding	19p13.11	-0.70	2.22e-35
Down	ENSG00000196754	S100A2	protein_coding	1q21.3	-0.69	8.93e-03
Down	ENSG00000085276	MECOM	protein_coding	3q26.2	-0.67	1.26e-04
Down	ENSG00000144810	COL8A1	protein_coding	3q12.1	-0.67	1.16e-10
Down	ENSG00000167772	ANGPTL4	protein_coding	19p13.2	-0.66	4.18e-08
Down	ENSG00000076716	GPC4	protein_coding	Xq26.2	-0.66	6.91e-13
Down	ENSG00000172594	SMPDL3A	protein_coding	6q22.31	-0.66	2.81e-08
Down	ENSG00000084734	GCKR	protein_coding	2p23.3	-0.66	7.12e-03
Down	ENSG00000129422	MTUS1	protein_coding	8p22	-0.65	5.50e-04
Down	ENSG00000137501	SYTL2	protein_coding	11q14.1	-0.65	9.12e-07
Down	ENSG00000164741	DLC1	protein_coding	8p22	-0.65	2.49e-06
Down	ENSG00000176871	WSB2	protein_coding	12q24.23	-0.65	4.82e-23
Down	ENSG00000154734	ADAMTS1	protein_coding	21q21.3	-0.65	2.03e-26
Down	ENSG00000157510	AFAP1L1	protein_coding	5q32	-0.64	5.33e-03
Down	ENSG00000171105	INSR	protein_coding	19p13.2	-0.64	1.29e-04
Down	ENSG00000124813	RUNX2	protein_coding	6p21.1	-0.63	4.49e-06
Down	ENSG00000128342	LIF	protein_coding	22q12.2	-0.63	4.54e-17
Down	ENSG00000103485	QPRT	protein_coding	16p11.2	-0.63	1.14e-21
Down	ENSG00000116016	EPAS1	protein_coding	2p21	-0.62	2.20e-10
Down	ENSG00000165105	RASEF	protein_coding	9q21.32	-0.62	1.80e-08
Down	ENSG00000077782	FGFR1	protein_coding	8p11.23	-0.62	1.55e-17
Down	ENSG00000163661	PTX3	protein_coding	3q25.32	-0.61	4.40e-05
Down	ENSG00000249855	EEF1A1P19	processed_pseudogene	5p12	-0.61	4.61e-03
Down	ENSG00000144824	PHLDB2	protein_coding	3q13.2	-0.61	4.67e-09
Down	ENSG00000164305	CASP3	protein_coding	4q35.1	-0.60	1.28e-10
Down	ENSG00000135447	PPP1R1A	protein_coding	12q13.2	-0.60	2.72e-03
Down	ENSG00000128340	RAC2	protein_coding	22q13.1	-0.59	1.86e-08

Caki2-sh*SPDL1* cells: Caki-2 cells stably transfected with shRNA against *SPDL1*; shCTRL cells: Caki-2 cells stably transfected with non-target shRNA control;

Table S5. Analysis of the PPI network properties using the Network Analyzer plugin in the Cytoscape software.

Name	Degree	Betweenness	Closeness	Clustering Coefficient	Stress	Average Shortest Path Length
ADAMTS1	1	0.000	0.281	0.000	0	3.564
IL6	28	0.154	0.389	0.241	6800	2.573
ADAMTSL3	2	0.018	0.166	0.000	590	6.036
TMEM45A	1	0.000	0.142	0.000	0	7.027
LTBP1	2	0.036	0.197	0.000	1176	5.064
ADCY5	4	0.070	0.211	0.333	2640	4.745
GNAO1	5	0.118	0.255	0.100	4554	3.927
GCKR	3	0.062	0.184	0.000	1992	5.445
PDE11A	2	0.000	0.175	1.000	0	5.727
PDE10A	3	0.008	0.208	0.667	536	4.818
AFAP1	2	0.058	0.257	0.000	1190	3.891
PLEK	7	0.120	0.325	0.238	2958	3.073
GMDS	3	0.047	0.214	0.000	996	4.673
AGR2	3	0.000	0.257	0.667	2	3.891
CEACAM6	2	0.000	0.256	1.000	0	3.900
EPCAM	11	0.089	0.343	0.327	3052	2.918
KRT8	4	0.005	0.286	0.500	202	3.500
ANGPTL4	4	0.000	0.295	1.000	0	3.391
CCL2	19	0.023	0.355	0.409	1636	2.818
EPAS1	9	0.001	0.320	0.750	116	3.127
TNF	30	0.352	0.410	0.214	12030	2.436
ANK1	6	0.103	0.329	0.133	2278	3.036
PIEZO2	1	0.000	0.248	0.000	0	4.027
KCNQ3	3	0.036	0.251	0.000	550	3.991
TIAM1	4	0.019	0.258	0.333	690	3.882
L1CAM	7	0.081	0.301	0.190	3076	3.327
ANKRD1	3	0.001	0.256	0.333	36	3.909

EGR1	13	0.083	0.337	0.321	4420	2.964
HEY2	3	0.001	0.270	0.667	74	3.709
RUNX2	9	0.014	0.320	0.500	1114	3.127
ANOS1	3	0.004	0.254	0.667	218	3.936
NLGN4X	6	0.029	0.247	0.267	1208	4.045
FGFR1	8	0.040	0.305	0.286	2342	3.282
AUTS2	4	0.008	0.253	0.500	314	3.945
NMUR2	5	0.039	0.299	0.300	1564	3.345
CNTN4	5	0.026	0.258	0.400	1014	3.882
PTPRD	6	0.055	0.267	0.133	2034	3.745
BAMBI	2	0.011	0.238	0.000	364	4.200
INSR	5	0.056	0.278	0.000	2680	3.600
FZD4	4	0.022	0.247	0.000	944	4.055
BCO2	1	0.000	1.000	0.000	0	1.000
STRA6	1	0.000	1.000	0.000	0	1.000
C7orf57	1	0.000	1.000	0.000	0	1.000
PRR15	1	0.000	1.000	0.000	0	1.000
CASP3	17	0.130	0.364	0.331	4586	2.745
PELI2	4	0.019	0.272	0.167	840	3.673
IGFBP4	3	0.000	0.303	1.000	0	3.300
CXCL8	22	0.071	0.362	0.312	3182	2.764
QPRT	3	0.054	0.272	0.000	1228	3.682
FGF13	13	0.050	0.353	0.462	2766	2.836
CD274	13	0.060	0.341	0.449	3052	2.936
RBFOX3	7	0.127	0.340	0.571	5186	2.945
RSAD2	4	0.000	0.299	1.000	0	3.345
GDF15	8	0.036	0.313	0.500	1458	3.200
IL32	4	0.000	0.299	1.000	0	3.345
TNFRSF9	7	0.001	0.321	0.810	118	3.118
PTX3	7	0.000	0.307	0.857	30	3.255
IL1R1	8	0.008	0.313	0.643	508	3.191
LIF	6	0.000	0.306	0.933	6	3.264
TNFAIP6	7	0.000	0.310	0.905	20	3.227
MTUS1	8	0.044	0.318	0.321	2238	3.145
SPDL1	**2**	**0.000**	**0.260**	**1.000**	**0**	**3.845**
CHGA	5	0.036	0.284	0.100	1314	3.527
SYT1	7	0.153	0.289	0.095	5598	3.455
CPE	1	0.000	0.221	0.000	0	4.518
SST	6	0.020	0.323	0.400	1146	3.100
CLDN11	3	0.018	0.232	0.333	584	4.318
INHBB	1	0.000	0.188	0.000	0	5.309
ESAM	2	0.000	0.231	1.000	0	4.327
CLDN2	4	0.054	0.298	0.333	1740	3.355
SEMA5A	2	0.000	0.206	1.000	0	4.845
COL5A1	5	0.123	0.243	0.000	4080	4.109
MXRA5	2	0.018	0.197	0.000	590	5.082
COL8A1	1	0.000	0.196	0.000	0	5.100
FSTL1	4	0.140	0.308	0.167	4856	3.245
NELL2	1	0.000	0.196	0.000	0	5.100
CPLX2	3	0.000	0.229	0.667	16	4.364
VAMP8	4	0.021	0.233	0.167	720	4.300
SYNGR1	2	0.000	0.225	1.000	0	4.436
CSRNP1	1	0.000	0.253	0.000	0	3.955
IRAK2	5	0.005	0.302	0.700	376	3.309
F2RL2	2	0.000	0.277	1.000	0	3.609
FLG	3	0.000	0.298	1.000	0	3.355
DLC1	1	0.000	0.242	0.000	0	4.136
DOC2A	2	0.018	0.215	0.000	412	4.655
DOC2B	1	0.000	0.177	0.000	0	5.645
DOCK8	3	0.011	0.248	0.333	534	4.036
RAC2	4	0.020	0.306	0.500	856	3.264
KANK1	2	0.000	0.200	0.000	2	5.009
MECOM	2	0.003	0.264	0.000	198	3.791
EMP1	1	0.000	0.239	0.000	0	4.191
MAL2	2	0.018	0.257	0.000	480	3.891
ESPN	1	0.000	0.214	0.000	0	4.664
GPC4	3	0.027	0.288	0.000	1332	3.473

PDGFD	2	0.002	0.245	0.000	96	4.082
FOXQ1	1	0.000	0.177	0.000	0	5.664
GABRE	1	0.000	0.232	0.000	0	4.318
GFPT2	2	0.021	0.190	0.000	560	5.264
SLC16A9	2	0.036	0.156	0.000	1216	6.400
S100A2	1	0.000	0.239	0.000	0	4.191
PPP2R5B	2	0.018	0.219	0.000	792	4.573
JRK	1	0.000	0.201	0.000	0	4.982
PHLDB2	2	0.007	0.247	0.000	296	4.045
KCNC3	1	0.000	0.201	0.000	0	4.982
KCNK5	1	0.000	0.667	0.000	0	1.500
KCNN4	2	1.000	1.000	0.000	2	1.000
SLC12A2	1	0.000	0.667	0.000	0	1.500
KMO	1	0.000	0.214	0.000	0	4.673
MALL	1	0.000	0.205	0.000	0	4.882
MDGA1	1	0.000	0.199	0.000	0	5.036
OLFML2B	1	0.000	0.165	0.000	0	6.073
NEDD9	1	0.000	0.211	0.000	0	4.736
PPP1R1A	1	0.000	0.180	0.000	0	5.564
RHOU	1	0.000	0.205	0.000	0	4.873
SCAMP5	1	0.000	0.225	0.000	0	4.445
SLC17A3	2	0.018	0.136	0.000	610	7.373
SLC47A1	1	0.000	0.120	0.000	0	8.364
SYTL2	1	0.000	0.189	0.000	0	5.291

Tabele S6. Summary of cohort clinical characteristics.

Vairable	TMA_1	TMA_2	TMA_3	TMA_4
Case number	106	114	86	79
Age				
Mean±SD	62.96±9.96	64±11.01	57.08±10.85	57.33±9.98
Median±IRQ	64±55.5-72	64.5±57.75-72	57.05±49-64.25	57±49-64
Sex				
Male	71	68	57	52
Female	35	46	29	27
Grade				
Gx	0	0	4	0
G1	16	4	43	42
G2	63	93	35	31
G3	19	13	4	6
G4	8	4	0	0
pT status				
T1	32	75	32	43
T2	29	18	38	30
T3	42	21	15	5
T4	3	0	1	1
c/pN status				
N0	99	112	85	77
N1	6	2	1	1
N2	1	0	0	1
c/pM status				
M0	106	112	85	75
M1	0	2	1	0

Abbreviations: c, clinical; p, pathological; TMA, tissue micro/macroarray; TMA_1, in-house tissue macroarray Jurasz/Bydgoszcz cohort; TMA_2, tissue macroarray Błażak/Inowrocław cohort; TMA_3 tissue microarray KD2085 cohort; TMA_4 tissue microarray KD2082a cohort. SD, standard deviation, IRQ, interquartile range.

Table S7. Missing data on testing variables in the TCGA cohort.

Variable	Case number (%)
Sex	0 (0)
Age	0 (0)
Grade	8 (1.60)
pT status	0 (0)
N status	0 (0)

M status	0 (0)
TNM stage	0 (0)
AS	28 (5.61)
FGA	3 (0.60)

Table S8. Details on the Gene Expression Omnibus (GEO) datasets.

GSE number	Sample size	Platform	Data retrieval	Authors/Citation(s)
GSE15641	32 clear cell RCC and 23 normal kidney samples	GPL96 [HG-U133A] Affymetrix Human Genome U133A Array	ShinyGEO	Jones J, Otu H, Spentzos D, Kolia S et al. Gene signatures of progression and metastasis in renal cell cancer. Clin Cancer Res 2005 Aug 15;11(16):5730-9
GSE16449	52 clear cell RCC tumors specimens and 18 corresponding non-tumor samples	GPL6480 Agilent-014850 Whole Human Genome Microarray 4x44K G4112F	ShinyGEO	Brannon AR, Reddy A, Seiler M, Arreola A et al. Molecular Stratification of Clear Cell Renal Cell Carcinoma by Consensus Clustering Reveals Distinct Subtypes and Survival Patterns. Genes Cancer 2010 Feb 1;1(2):152-163
GSE66272	27 clear cell RCC tumor specimens and 26 corresponding non-tumor samples	GPL570 [HG-U133_Plus_2] Affymetrix Human Genome U133 Plus 2.0 Array	ShinyGEO	Wotschofsky Z, Gummlich L, Liep J, Stephan C et al. Integrated microRNA and mRNA Signature Associated with the Transition from the Locally Confined to the Metastasized Clear Cell Renal Cell Carcinoma Exemplified by miR-146-5p. PLoS One 2016;11(2):e0148746
GSE71963	32 clear cell RCC tumor specimens and 16 normal kidney tissues	GPL6480 Agilent-014850 Whole Human Genome Microarray 4x44K G4112F	ShinyGEO	Liep J, Kilic E, Meyer HA, Busch J et al. Cooperative Effect of miR-141-3p and miR-145-5p in the Regulation of Targets in Clear Cell Renal Cell Carcinoma. PLoS One 2016;11(6):e0157801
GSE11151	26 clear cell RCC tumor specimens and 5 normal kidneys	GPL570 [HG-U133_Plus_2] Affymetrix Human Genome U133 Plus 2.0 Array	TidyGEO	Takahashi M, Tsukamoto Y, Kai T, Tokunaga A et al. Downregulation of WDR20 due to loss of 14q is involved in the malignant transformation of clear cell renal cell carcinoma. Cancer Sci 2016 Apr;107(4):417-23 Yusenko MV, Kuiper RP, Boethe T, Ljungberg B et al. High-resolution DNA copy number and gene expression analyses distinguish chromophobe renal cell carcinomas and renal oncocytomas. BMC Cancer 2009 May 18;9:152 Yusenko MV, Zubakov D, Kovacs G. Gene expression profiling of chromophobe renal cell carcinomas and renal oncocytomas by Affymetrix GeneChip using pooled and individual tumours. Int J Biol Sci 2009 Jul 29;5(6):517-27
GSE40435	101 pairs of ccRCC tumours and adjacent non-tumour renal tissue	GPL10558, Illumina HumanHT-12 V4.0 expression beadchip	TidyGEO	Wozniak MB, Le Calvez-Kelm F, Abedi-Ardekani B, Byrnes G et al. Integrative genome-wide gene expression profiling of clear cell renal cell carcinoma in Czech Republic and in the United States. PLoS One 2013;8(3):e57886.
GSE53757	72 clear cell renal cell carcinoma tissue and 72 matched normal kidney tissue	GPL570, [HG-U133_Plus_2] Affymetrix Human Genome U133 Plus 2.0 Array	TidyGEO	von Roemeling CA, Radisky DC, Marlow LA, Cooper SJ et al. Neuronal pentraxin 2 supports clear cell renal cell carcinoma by activating the AMPA-selective glutamate receptor-4. Cancer Res 2014 Sep 1;74(17):4796-810.

GSE36895	29 clear cell RCC tumor specimens and 23 adjacent non-tumor samples	GPL570, [HG-U133_Plus_2] Affymetrix Human Genome U133 Plus 2.0 Array	TidyGEO	Peña-Llopis S, Vega-Rubín-de-Celis S, Liao A, Leng N et al. BAP1 loss defines a new class of renal cell carcinoma. Nat Genet 2012 Jun 10;44(7):751-9. Peña-Llopis S, Brugarolas J. Simultaneous isolation of high-quality DNA, RNA, miRNA and proteins from tissues for genomic applications. Nat Protoc 2013 Nov;8(11):2240-55.
GSE46699	67 clear cell RCC tumor specimens and 63 adjacent non-tumor samples	GPL570, [HG-U133_Plus_2] Affymetrix Human Genome U133 Plus 2.0 Array	TidyGEO	Eckel-Passow JE, Serie DJ, Bot BM, Joseph RW et al. ANKS1B is a smoking-related molecular alteration in clear cell renal cell carcinoma. BMC Urol 2014 Jan 31;14:14. Eckel-Passow JE, Serie DJ, Bot BM, Joseph RW et al. Somatic expression of ENRAGE is associated with obesity status among patients with clear cell renal cell carcinoma. Carcinogenesis 2014 Apr;35(4):822-7.
GSE22541	24 primary tumors of clear-cell renal cell carcinoma (ccRCC)	GPL570, [HG-U133_Plus_2] Affymetrix Human Genome U133 Plus 2.0 Array	TidyGEO	Wuttig D, Zastrow S, Füssel S, Toma MI et al. CD31, EDNRB and TSPAN7 are promising prognostic markers in clear-cell renal cell carcinoma revealed by genome-wide expression analyses of primary tumors and metastases. Int J Cancer 2012 Sep 1;131(5):E693-704.
GSE100666	3 ccRCCs and 3 corresponding adjacent normal tissues	GPL1695, Phalanx Human OneArray Ver. 6 Release 1	ShinyGEO	Peng Z, He J, Zheng J, Microarray expression profiling of dysregulated mRNAs between ccRCC tumor tissues and corresponding adjacent normal tissues